

## THE GENERATION OF AVAILABLE POTENTIAL ENERGY BY LATENT HEAT RELEASE IN A MID-LATITUDE CYCLONE

BEN R. BULLOCK<sup>1</sup> and DONALD R. JOHNSON

Department of Meteorology, The University of Wisconsin, Madison, Wis.

### ABSTRACT

The theory of available potential energy applied to a "translating" atmospheric volume is used to estimate the generation of available potential energy for the cyclogenetic, mature, and occluding stages of a mid-latitude cyclone. Primary attention is focused upon the importance of the diabatic process of latent heat release in generating the storm's available potential energy. In addition, preliminary estimates for the process of infrared cooling are presented.

Total latent heat release is determined from observed precipitation rates. Three different models for the vertical distribution of latent heat release together with the storm's structure provided by isentropic analyses are utilized to estimate the contribution by latent heat release to the available potential energy of the disturbance. For each stage of the storm, variations in the generation estimates between models were extremely small. For the cyclogenetic, mature, and occluding stages, generation estimates of approximately 1, 8, and 6  $W m^{-2}$ , respectively, reflected changes in the horizontal distribution of precipitation about the storm.

Two simplified cooling distributions were assumed to evaluate the importance of infrared cooling in the generation. The first was one of uniform cooling at the rate of  $1.4^{\circ}C day^{-1}$  throughout the volume, and the second was one in which the clear air was cooled at a greater rate than the cloudy air. Positive generation estimates on the order of 1 to 2  $W m^{-2}$  resulted from these calculations.

The results of this study indicate that the diabatic process of latent heat release is very likely an important factor in the subsequent behavior of the system. It is speculated that an energy supply of this magnitude, available for immediate conversion to kinetic energy, is sufficient to offset a major portion of the storm's frictional dissipation. Generation estimates for the process of infrared cooling, while less reliable than those for latent heat release, indicate that this process also contributes to the storm's available potential energy supply.

### 1. INTRODUCTION

In contrast to earlier theories of the general circulation envisioning one or more meridional cells, atmospheric scientists have rejected this simplified view and emphasized the importance of the atmosphere's quasi-horizontal motion in satisfying the required heat and momentum transport for the global scale. The general circulation theory formulated during the last two decades and summarized by Lorenz (1967) is based upon evidence that the "nonzonal inequalities" are the principal site of the conversion of atmospheric potential energy to kinetic energy (Starr 1958). According to this theory, the east-west thermal contrast within the migratory systems represents available potential energy that is converted to kinetic energy through the process of rising warm air and sinking cold air.

The importance of the adiabatic conversion of available potential energy to kinetic energy within the cyclones and anticyclones is a central feature of this theory. Recently, however, the importance of diabatic effects, in particular latent heat release, within the cyclonic circulations is being realized. Investigations by Aubert (1957), Eliassen (1962), Rao (1966), and others have emphasized the contribution of released latent heat to the vertical motion field, while Danard (1964, 1966) has shown that this process contributes to available potential energy production and an increased rate of energy conversion during the mature stage of a cyclone. These results support Petterssen's (1960) belief that it is not reasonable to treat the mobile weather systems as manifestations of adiabatic processes while simultaneously searching for energy sources and sinks to account for the general circulation of which these systems are an integral part.

<sup>1</sup> Now affiliated with the Department of Earth Science, Edinboro State College, Edinboro, Pa.

To provide a better understanding of the importance of diabatic processes within the energetics of cyclones, this study focuses primary attention on the distribution of released latent heat in producing energy available for conversion to kinetic energy within the scale of these systems. Brief consideration is also given to its production by the process of infrared emission.

The generation of available potential energy by the release of latent heat is studied using models approximating the vertical heating distribution. The total latent heat release in the vertical is determined from the surface precipitation rate, while the distribution of heating is specified by relating variations in the condensation rate to models of vertical motion. These heating models and the atmospheric structure provided by isentropic analyses are used to estimate the generation of available potential energy for the developing, mature, and early occluding stages of a mid-latitude cyclone. The generation by infrared radiative processes is obtained from assumed infrared cooling distributions. This approach provides an estimate of the in situ generation of the storm's available potential energy. The boundary layer frictional dissipation is also estimated to contrast the relative importance of the storm's energy source by diabatic processes with its sink by frictional effects.

## 2. BASIC ENERGY EQUATIONS

Following Margules (1903), Lorenz (1955) defined available potential energy as the sum of the internal and gravitational potential energy in the actual atmosphere minus the sum of these energies after an adiabatic mass redistribution of the global atmosphere to a horizontal, statically stable density stratification. The atmospheric configuration achieved by this hypothetical redistribution is commonly called the reference state.

Unfortunately, available potential energy theory based upon a global reference state does not provide a firm basis for energy studies of smaller scales of atmospheric motion. Because the most intense conversion of available potential energy to kinetic energy occurs in the migratory cyclones and anticyclones of middle latitudes, budget studies of this scale of motion are necessary for a proper understanding of their role in the general circulation. The theoretical basis for such studies has been provided recently by Johnson (1970), who has developed budget equations for the available potential energy of a storm by defining a reference state for a volume surrounding and moving with the disturbance. Within this volume, the storm's available potential energy is

$$\bar{A} = \bar{\pi} - \bar{\pi}_r \quad (1)$$

where  $\pi$  and  $\pi_r$  are respectively the total potential energy (internal plus gravitational) in the existing atmosphere and the reference state. The overbar represents the

area average of a quantity, and the subscript  $r$  represents the value of a quantity in the reference state.

The time rate of change of the storm's available potential energy is

$$\frac{d\bar{A}}{dt} = \frac{d\bar{\pi}}{dt} - \frac{d\bar{\pi}_r}{dt} \quad (2)$$

that shows the dependence on the changes of the actual and reference state energies in the translating volume. From Johnson (1970), the rate of change of the storm's available potential energy is

$$\frac{d\bar{A}}{dt} = \bar{G} - \bar{C}(A, K) + \bar{B} \quad (3)$$

where  $G$  is the generation of available potential energy by diabatic processes,  $C(A, K)$  is the rate of conversion of available potential energy to kinetic energy, and  $B$  is the change of available potential energy produced by pressure work on and relative advection through the boundary of the translating volume. The major differences between the available potential energy expressions for a global or storm budget are the boundary term and the redefined reference state. If the volume is extended to include the entire atmosphere, the boundary term vanishes, and the generation and conversion correspond to the global expressions derived by Dutton and Johnson (1967). In this study, only the generation of the storm's available potential energy is determined.

In isentropic coordinates, the generation of the storm's available potential energy is

$$\bar{G} = \int_{\theta_0}^{\theta_r} \overline{\epsilon \rho J_\theta Q_m} d\theta \quad (4)$$

where  $\rho$  is density,  $Q_m$  is the rate of specific heat addition,  $\theta_0$  and  $\theta_r$  are the atmosphere's minimum and maximum potential temperatures, respectively.  $J_\theta$  is the transformation Jacobian  $|\partial z / \partial \theta|$ . The efficiency factor in eq (4) is

$$\epsilon = 1 - \left( \frac{p_r}{p} \right)^\kappa \quad (5)$$

where  $\kappa$  is the ratio of the gas constant  $R$  to the specific heat at constant pressure  $c_p$  and  $p_r$  is the reference pressure of an isentropic surface. Under the hydrostatic assumption, the reference pressure  $p_r$  may be evaluated by area-averaging the atmospheric pressure on an isentropic surface (Dutton and Johnson 1967).

In diagnostic energy studies of the effects of diabatic heating, the efficiency factor is an important element. It is a measure of the condition that for diabatic processes the change of total potential energy in the actual atmosphere may differ from that in the reference atmosphere. Examination of eq (2) shows that available potential energy is produced when the change of atmospheric total

potential energy exceeds the change of the reference atmosphere's total potential energy. A positive (negative) generation results when heating (cooling) occurs at pressures higher and cooling (heating) at pressures lower than the reference pressure.

In this study, the spatial distribution of efficiency factors is obtained from isentropic analyses of a mid-latitude cyclone, while observed surface precipitation rates are used to establish total latent heat release. Models developed in the next section, which approximate the vertical distribution of latent heat release, are then used in estimating the generation.

### 3. MODELS OF LATENT HEAT RELEASE

Latent heat release by the condensation process represents the sink of water vapor within the storm, while sources of water vapor are primarily from low-level advection of warm moist air from oceanic areas into the storm. The relation between the storm's water vapor sources, sinks, and storage is first developed in a water vapor budget equation before modeling the latent heat release.

#### THE WATER VAPOR BUDGET EQUATION

The development of a water vapor budget equation for a volume moving with the storm is based on the generalization of the Leibnitz rule for the differentiation of integrals. In general, the total water vapor mass in an arbitrary volume defined in pressure coordinates is

$$Q = \int_{V_p} q \rho J_p dV_p \quad (6)$$

where  $q$  is the specific humidity,  $J_p$  is the transformation Jacobian  $|\partial z / \partial p|$  and  $V_p$  is the volume of integration bounded by vertical walls and lower and upper pressure surfaces  $p_1$  and  $p_2$ . The differential  $dV_p$  is equal to  $dp dx dy$ . From the generalization of the Leibnitz rule to three dimensions, the time rate of change of the storm's water vapor mass is

$$\frac{dQ}{dt} = \int_{V_p} \left[ \frac{\partial}{\partial t} (q \rho J_p) + \nabla_p \cdot (q \rho J_p \mathbf{W}) + \frac{\partial}{\partial p} (q \rho J_p \omega_B) \right] dV_p \quad (7)$$

where again  $\mathbf{W}$  is the lateral boundary velocity and  $\omega_B$  is the velocity of the vertical boundary with respect to the vertical pressure coordinate.

By substituting the continuity equation in pressure coordinates

$$\frac{d}{dt} (\rho J_p) + \rho J_p \left( \nabla_p \cdot \mathbf{U} + \frac{\partial \omega}{\partial p} \right) = 0 \quad (8)$$

into eq (7), the budget equation becomes

$$\frac{dQ}{dt} = \int_{V_p} \left\{ \rho J_p \frac{dq}{dt} + \nabla_p \cdot [q \rho J_p (\mathbf{W} - \mathbf{U})] + \frac{\partial}{\partial p} [q \rho J_p (\omega_B - \omega)] \right\} dV_p \quad (9)$$

where  $\omega$  is the fluid vertical velocity in pressure coordinates.

From use of the divergence theorem, the budget equation for the storm's water vapor mass is

$$\frac{dQ}{dt} = \int_A \int_{p_2}^{p_1} \rho J_p \frac{dq}{dt} dp dA - \int_{p_2}^{p_1} \int_L q \rho J_p (\mathbf{U} - \mathbf{W}) \cdot \mathbf{n} dL dp + \int_S \{ [q \rho J_p (\omega - \omega_B)]_{p_2} - [q \rho J_p (\omega - \omega_B)]_{p_1} \} dS. \quad (10)$$

The lower vertical boundary of the volume will be the surface of the earth. This condition is maintained by equating  $p_1$  to  $p_0$  and  $\omega_B(x, y, p_0, t)$  to  $\omega(x, y, p_0, t)$ . Thus the fluid always remains in contact with the earth's surface. Now, by defining the relative velocity of the fluid,  $\mathbf{U}_r$ , to be the difference between  $\mathbf{U}$  and  $\mathbf{W}$  and letting the upper surface of the volume be a fixed pressure surface [so that  $\omega_B(p_2)$  vanishes], the storm's water vapor budget equation becomes

$$\frac{dQ}{dt} = \int_A \int_{p_2}^{p_0} \rho J_p \frac{dq}{dt} dp dA - \int_{p_2}^{p_0} \int_L \mathbf{n} \cdot (q \rho J_p \mathbf{U}_r) dL dp + \int_S (q \rho J_p)_{p_2} \omega_2 dS.$$

From the hydrostatic assumption and the expression

$$\frac{dq}{dt} = \omega \frac{dq}{dp}, \quad (11)$$

the final budget equation for the storm's water vapor mass is

$$\frac{dQ}{dt} = \frac{1}{g} \int_A \int_{p_2}^{p_0} \omega \frac{dq}{dp} dp dA - \frac{1}{g} \int_{p_2}^{p_0} \int_L \mathbf{n} \cdot q \mathbf{U}_r dL dp + \frac{1}{g} \int_S q_2 \omega_2 dS. \quad (12)$$

The first term in eq (12) represents sources and sinks by evaporation and condensation of water vapor within the moving volume and will be denoted by  $S(Q)$ . The last two terms measure the flux of water vapor through the lateral boundary by the relative velocity of the fluid and by vertical advection through the volume's upper surface. If the volume is extended to the top of the atmosphere, the last term also vanishes under the condition that  $\omega(0)$  is zero.

In this study, the generation of available potential energy by the release of latent heat is emphasized. Thus, only the sink of water vapor by the process of condensation

is considered. In a mature storm, the water vapor storage tends to be constant, such that the sink by condensation is primarily balanced by lateral inflow in the low troposphere. Vertical advection through the upper surface must be small for budget volumes extending into the stratosphere or high troposphere.

In all three models employed in this study, it is assumed that condensation occurs for upward vertical motion when  $q$  is equal to  $q_s$ . Thus, the change of water vapor mass in the subregion of the source integral where these conditions are satisfied is

$$S(Q_s) = \frac{1}{g} \int_{A_s} \int_{p_{2s}}^{p_{1s}} \omega \frac{dq_s}{dp} dp dA_s \quad \{q = q_s; \omega < 0\} \quad (13)$$

where the subscript  $s$  denotes the condition of saturation and the pressures  $p_{1s}$  and  $p_{2s}$  denote the lower and upper boundary pressures for the precipitating portion of the volume.

Under the assumption that all the condensed water vapor precipitates immediately, the relation between  $S(Q_s)$  and the precipitation rate is

$$S(Q_s) = - \int_{A_s} \rho_w \dot{P} dA_s \quad (14)$$

where  $\dot{P}$  is the rate of precipitation ( $\text{cm hr}^{-1}$ ),  $\rho_w$  is the density of water, and  $A_s$  is the area of the precipitating region.

By combining eq (13) and (14) and using the knowledge that the precipitation rate is a measure of the rate of latent heat release, the total heating in the region defined for  $S(Q_s)$  is

$$H_L(S) = \int_{A_s} L_{lv} \rho_w \dot{P} dA_s = - \frac{1}{g} \int_{A_s} \int_{p_{2s}}^{p_{1s}} L_{lv} \omega \frac{dq_s}{dp} dp dA_s \quad (15)$$

where  $L_{lv}$  is the latent heat of condensation. Note the integrand of eq (15), a function of the vertical motion distribution and the individual change of specific humidity with pressure, is equal to the latent heating component of  $Q_m$ . In the next section, three models of latent heat release are developed to estimate the spatial distribution of latent heat release in the cyclone.

#### PHYSICAL MODELING

Models for the vertical distribution of latent heat release are obtained by assuming different profiles of the vertical motion and the individual change of specific humidity with pressure that satisfy the integral constraint of eq (15). Each model utilizes the observed surface precipitation rate to establish the total latent heat release in the atmospheric column.

In the models, heat is distributed between the lifting condensation level  $p_{1s}$  and an assumed cloud top level corresponding to the upper boundary of the precipitating volume  $p_{2s}$ . Examination of soundings at stations reporting steady precipitation showed close agreement between the lifting condensation level and the observed cloud bases. However, because cloud tops are not easily determined from soundings, several different cloud top levels are selected to study the influence of various heating profiles in the estimates for the generation of available potential energy.

*First model of latent heat release.* Bradbury (1957) and others have shown that the major flux of moisture into extratropical cyclones occurs below 800 mb. Because the equivalent potential temperature of air below 800 mb tends to be constant due to mixing in the boundary layer, Bradbury's result supports the assumption of a constant equivalent potential temperature for the first model. Thus, the moist adiabat through the lifting condensation level (LCL) defines the profile of the individual change of specific humidity. It is also assumed in the first model that the vertical velocity from the LCL to the cloud top is constant. The observed precipitation rate at the surface and the assumed cloud top uniquely determine the value of the vertical motion necessary to satisfy eq (15).

Typical profiles of vertical motion and latent heat release from this model are shown in figure 1A. The small heating maximum in the middle troposphere is associated with the maximum value of  $dq_s/dp$  on the pseudoadiabat.

*Second model of latent heat release.* The assumption of constant vertical motion made in the first model, though not unreasonable for shallow saturated layers, is not representative of large-scale vertical velocities over any substantial vertical extent of the atmosphere. In the second model, the vertical motion profile is assumed to be quadratic between the earth's surface and the cloud top, while the assumption of constant equivalent potential temperature for the ascending air is retained. A quadratic form for the vertical motion is

$$\omega = \omega_m (1 - X^2) \quad (16)$$

where  $\omega_m$  is the maximum upward vertical velocity at  $X$  equal to zero. The scaled pressure variable is

$$X = \frac{p - \frac{1}{2}(p_{2s} + p_0)}{\frac{1}{2}(p_{2s} - p_0)} \quad \begin{matrix} p_0 \geq p \geq p_{2s} \\ -1 \leq X \leq +1 \end{matrix} \quad (17)$$

where  $p_0$  and  $p_{2s}$  are the surface and the cloud top pressures, respectively.

Figure 1B presents the profiles of vertical motion and latent heat release from the second model for the same initial data used in the first model. Note that the heating maximum in the middle troposphere for the second model is substantially greater than the first model.

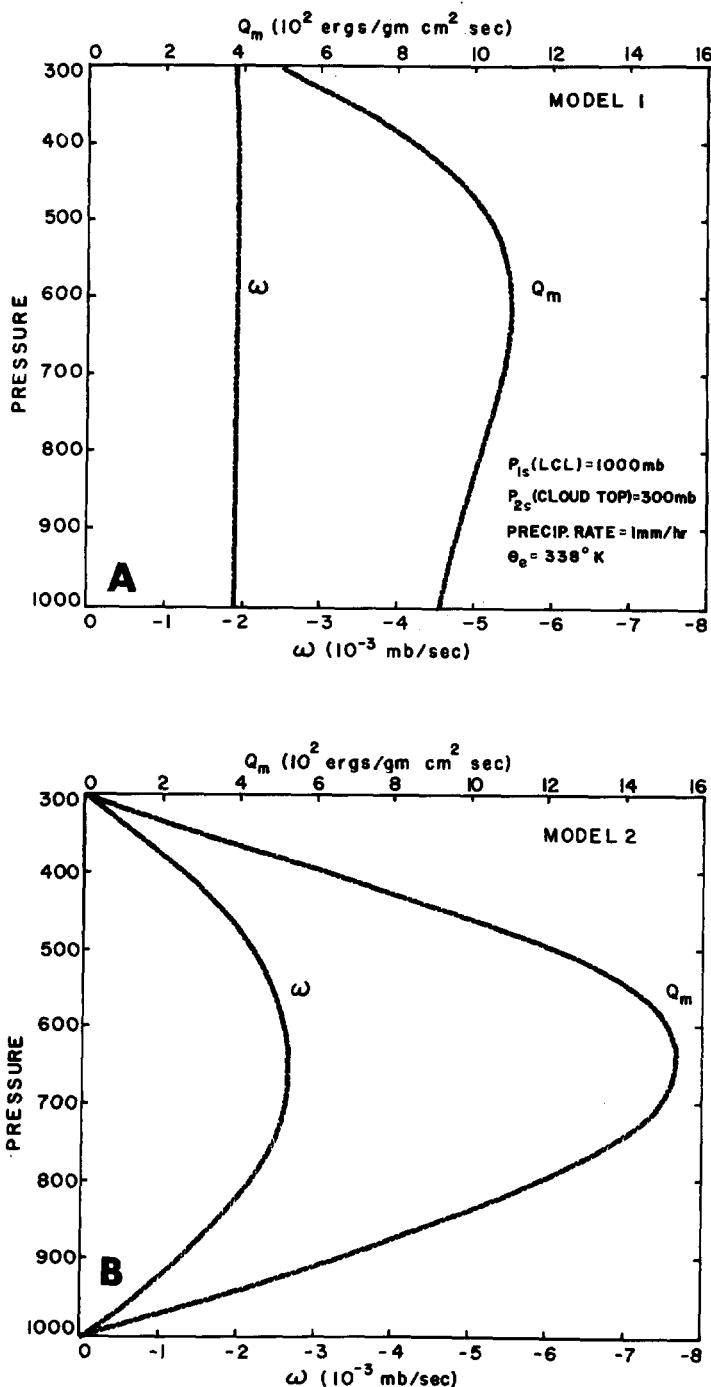


FIGURE 1.—Profiles of vertical motion and latent heat release for (A) model 1 and (B) model 2. Parameters for both models are indicated in the lower left corner of (A).

*Third model of latent heat release.* The assumption of constant equivalent potential temperature made in the previous two models implies that the lapse rate in the saturated portion of the column is moist adiabatic. Examination of soundings with deep saturated layers producing precipitation shows departures from this condition. In the third model, vertical variations in the equivalent potential temperature are allowed, while using the quadratic model-

ing of the vertical motion. The assumption of saturation on isentropic surfaces above the LCL but below the cloud top level together with pressure analyses of these surfaces determines the spatial distribution of equivalent potential temperature.

The vertical distribution of heating from the second and third models is quite similar. However, in the stable atmosphere, the third model releases more heat in the upper portion of the atmosphere than the second model because the equivalent potential temperature is assumed to increase with height.

#### 4. COMPUTATIONAL PROCEDURES

##### PRECIPITATION RATE AND LATENT HEAT ADDITION

Precipitation rates used to establish the latent heating distribution were obtained from hourly amounts recorded at several hundred stations throughout the United States. At each location, an average precipitation rate for a 4-hr period was determined. The area distribution of precipitation for a  $1^\circ$  grid was obtained by averaging the station data lying within a  $0.6^\circ$  latitude radius of each grid point. The objectively analyzed field using this scheme compared favorably with a subjective analysis.

Obviously, some error is made when using rainfall amounts to estimate latent heat release, since condensation can occur without precipitation. Wexler and Atlas (1958) state, however, that cloud storage of liquid water is small, especially in stratiform clouds producing precipitation and need not be considered in the calculation of rainfall rates. This indicates that errors in latent heat estimates induced by condensation without precipitation are minimal and the vertical profile of heating may be determined by using the total latent heat release based on the precipitation rate. The finite estimate of the latent heating per unit mass corresponding to the condensation rate at the  $i$ th grid point on the  $k$ th isentropic surface is

$$Q_{m,ik} = -L_{iv}\omega_{ik} \left( \frac{dq_s}{dp} \right)_{ik} \quad (18)$$

##### EFFICIENCY FACTOR

The efficiency factors were obtained from 10 isentropic surfaces equally spaced at  $5^\circ K$  intervals from  $280^\circ$  to  $325^\circ K$ . In computing the efficiency factor, the reference pressure  $p_r(\theta_k)$  was obtained for a circular volume with a 1700-km radius centered about the storm; and on underground portions of isentropic surfaces (Lorenz 1955), the pressure was set equal to the surface pressure. The grid-point estimate of the efficiency factor is

$$\epsilon_{ik} = 1 - \left( \frac{p_{rk}}{p_{ik}} \right)^\kappa \quad (19)$$

### GENERATION

Under the hydrostatic assumption, the finite approximation of the generation of available potential energy is

$$G = \frac{1}{g} \sum_{k=1}^{10} \sum_{i=1}^n G_{ik} \Delta p_{ik} \quad (20)$$

where  $n$  is the number of grid points and  $\Delta p_{ik}$  is one-half the difference between  $p_{k-1}$  and  $p_{k+1}$ . The generation estimate at each  $ik$ th point is

$$G_{ik} = \epsilon_{ik} Q_{m_{ik}} \quad (21)$$

### FRICTIONAL DISSIPATION

Frictional dissipation estimates for the planetary boundary layer are obtained using Lettau's (1961) formulation. The dissipation at the  $i$ th grid point is

$$D_i = \rho_i C_{\alpha_i}^2 U_{\sigma_i}^3 \cos \alpha \quad (22)$$

where  $U_{\sigma}$  is the geostrophic wind and  $\alpha$  is the angular departure of the geostrophic wind vector from the surface shear stress. The geostrophic drag coefficient (Kung 1963) is

$$C_{\alpha_i} = k [\ln(U_{\sigma_i}/z_0 f_i) - 1.865]^{-1} \quad (23)$$

where  $k$  is the von Kármán constant equal to 0.4,  $z_0$  is the roughness parameter, and  $f$  is the Coriolis parameter. In this study,  $z_0$  was assumed to be 50 cm, a representative value for the geographical region of the storm (Kung 1963), and  $\alpha$  was assumed to be 20°.

## 5. THE CASE STUDY

### SYNOPTIC DESCRIPTION

The cyclone selected for study developed rapidly on Mar. 25–26, 1964. The surface and 300°K isentropic analyses for three successive stages of the storm are presented in figure 2. At 1200 GMT on the 25th, the cyclone was located in northern Arkansas and southern Missouri along a frontal zone associated with strong low-level northward advection of warm, moist subtropical air ( $mT$ ) from the Gulf of Mexico and southward advection of continental polar air ( $cP$ ) from the northern Plains States.

The region of lowest pressure on the 300°K isentropic surface at 1200 GMT on the 25th shows that the coldest air was situated over Colorado and Wyoming. A strong baroclinic zone, indicated by the large gradient of pressure, was located to the rear of the developing depression. Above the baroclinic zone, 500-mb winds attained speeds of 80 kt in a portion of the jet core extending from northern Texas to Iowa.

By 0000 GMT on the 26th (fig. 2C), the cyclone was well developed and was moving northeastward at about 30 kt while deepening at the rate of approximately 1 mb hr<sup>-1</sup>. The vertical axis of the system still sloped to the west, with the 500-mb trough extending from the Dakotas to western Texas. The baroclinic zone (fig. 2D) that was located west

of the surface position of the cyclone had intensified. The 500-mb winds in excess of 90 kt extended from Oklahoma to northern Illinois.

By 1200 GMT on the 26th (fig. 2E), the system had just begun to occlude after reaching southern Ontario. A closed Low on the 500-mb surface centered over Lake Michigan indicated that the axis of the system was now nearly vertical. The 300°K isentropic analysis (fig. 2F) shows the baroclinic zone extending from directly over the surface system to the southwest. This is to be contrasted with its location well to the west of the Low during the cyclogenetic (March 25 1200 GMT) and mature (March 26 0000 GMT) stages. Again, the maximum 500-mb wind region extending from Tennessee to southern Ontario was situated above the 300°K baroclinic zone.

### VERTICAL AND HORIZONTAL DISTRIBUTION OF EFFICIENCY FACTORS

The generation of the storm's available potential energy is a function of the diabatic heating field and thermodynamic structure. The latter is implicitly manifested in the efficiency factor distribution. The pressure analysis on 10 isentropic surfaces was utilized to provide the efficiency factor distribution because isobars are also isolines of efficiency factors. In figures 2B, 2D, and 2F, efficiency factors for the 1700-km radial area corresponding to the isobars are presented in parentheses. The pressure analysis, primarily indicating the vertical displacement of the isentrope from low-tropospheric subtropical air to high-tropospheric polar air illustrates the relationship between thermal structure, efficiency factors, and regions where net heating and cooling generate available potential energy.

The reference pressure, also the area-averaged pressure for the storm, is presented in figure 3. As the storm evolved and moved northeastward, the reference pressure for all the isentropic surfaces decreased due to the relative inward flux of  $cP$  air and outward flux of  $mT$  air at the lateral boundary. Note in figures 2B, 2D, and 2F the decrease in reference pressure with time for the 300°K surface resulted in increasing the positive efficiency factors at high pressures in the subtropical air but decreasing the magnitude of the negative efficiencies at low pressures in the polar air.

Cross sections of potential temperature and efficiency factors along latitude circles were also prepared to study the time and vertical variation of efficiency factors within all stages of the storm. However, only three cross sections through the mature stage are presented in figure 4. For their position with respect to the storm center, refer to figure 2C. The cross sections show that the largest positive values occur at about 750 mb southeast of the surface low-pressure center, while the largest negative values occur at the 300-mb level in the polar troposphere northwest of the surface frontal zone. The three cross sections portray the contraction of the positive efficiency area and expansion of the negative area as one moves northward.

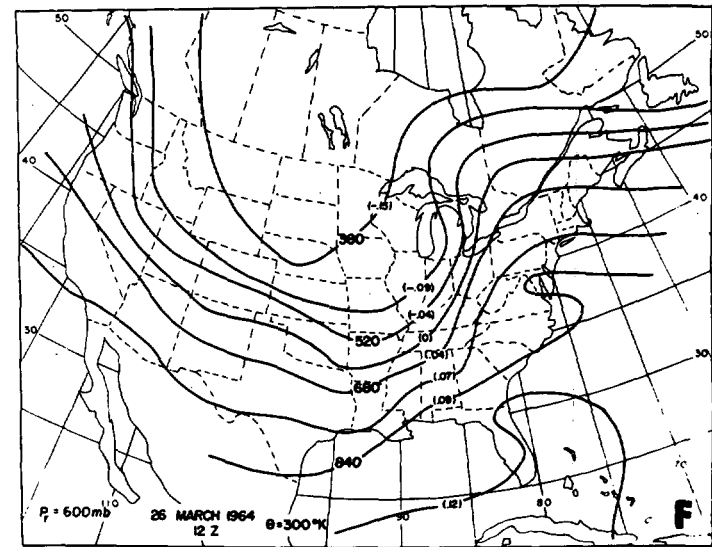
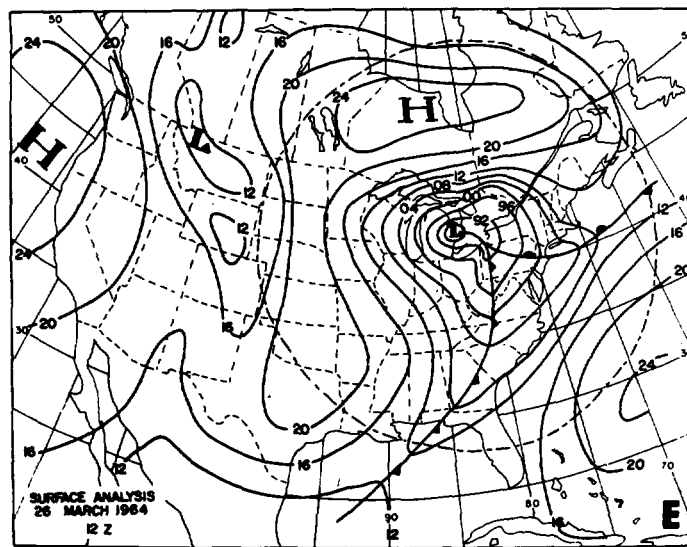
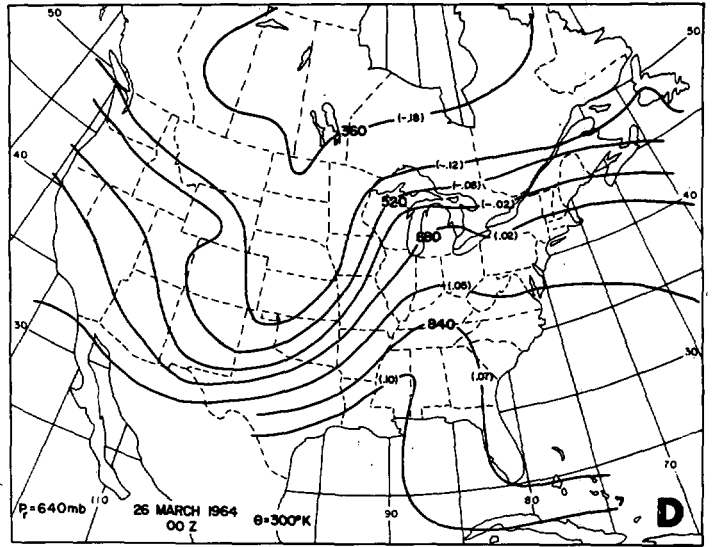
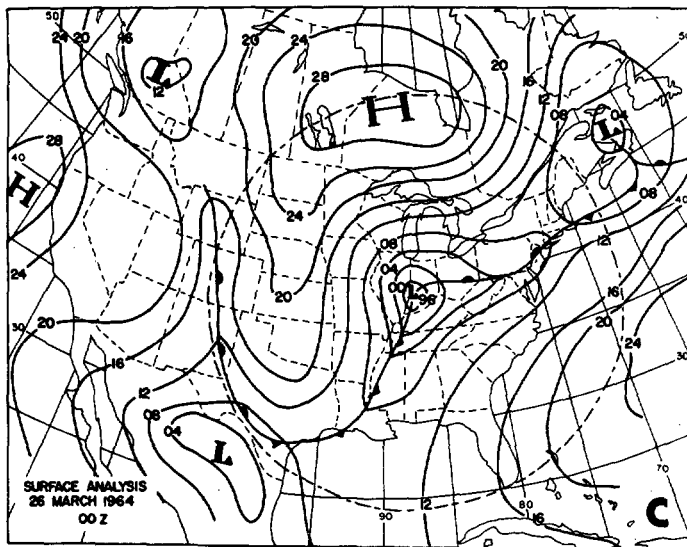
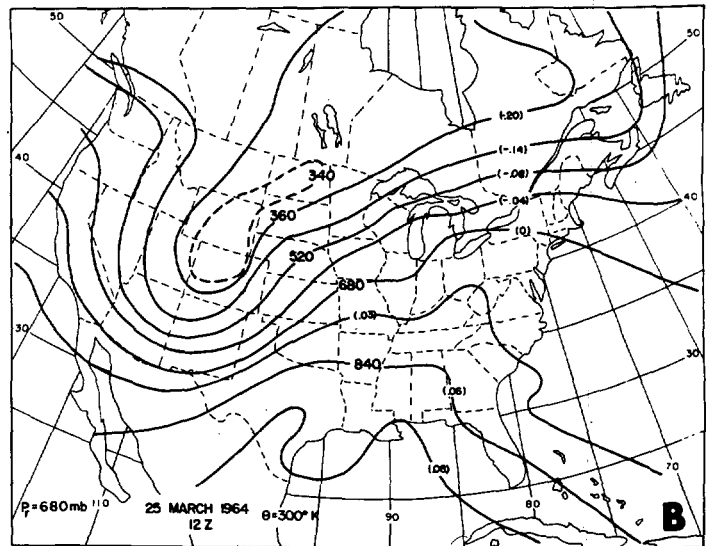
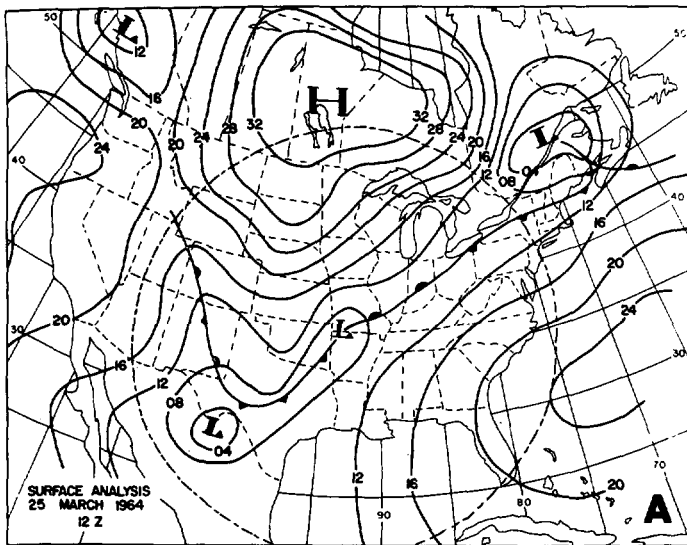


FIGURE 2.—Surface analyses for the cyclogenetic, mature, and occluded stages are presented in (A), (C), and (E). The dashed circular line outlines the region of the storm for which the generation was estimated. Pressure analyses (in mb) on the 300°K surface for the three stages are presented in (B), (D), and (F). The values of the efficiency factor isopleth for the 1700-km area that corresponds to the isobars are indicated in parentheses.

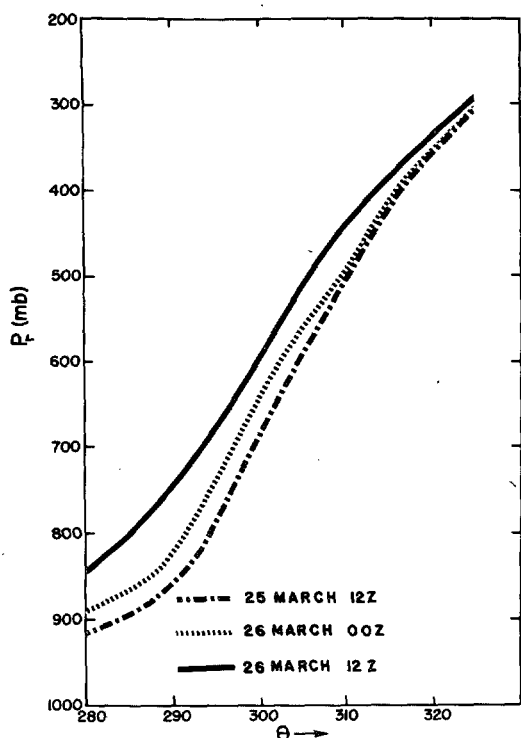


FIGURE 3.—Vertical profile of the reference pressure for the three stages of the storm.

While the same general features prevailed in the cross sections for both the developing and occluding stages, there were some differences. During the 24-hr period, the positive values in the subtropical air increased, and the absolute values of the efficiency factors in the polar air decreased. This tendency was related to the decrease in reference pressures as the storm evolved (fig. 3).

The cross sections and the  $300^{\circ}\text{K}$  isentropic analyses for all stages of the storm show that the zero efficiency factor isoline approximately coincides with the location of a major precipitation area commonly located north of the Low center. Released latent heat in these regions would therefore contribute to very small or even negative generation. In contrast, the peripheral areas of the cyclone where efficiency factors attain their largest absolute values are the regions where diabatic processes assume greater importance in the generation of available potential energy for the storm.

Another interesting feature noted in the evolution of the efficiency structure is the tendency for the zero efficiency isopleth to be more horizontal in the early stage and more vertical in the mature and occluded stage. In considering the effects of total heating, the efficiency structure indicates that low tropospheric heating and high tropospheric cooling are more efficient mechanisms in generating available potential energy in the cyclogenetic stage and that horizontal differential heating will become more efficient in the subsequent stages. A similar evolution was noted by Hahn and Horn (1969).

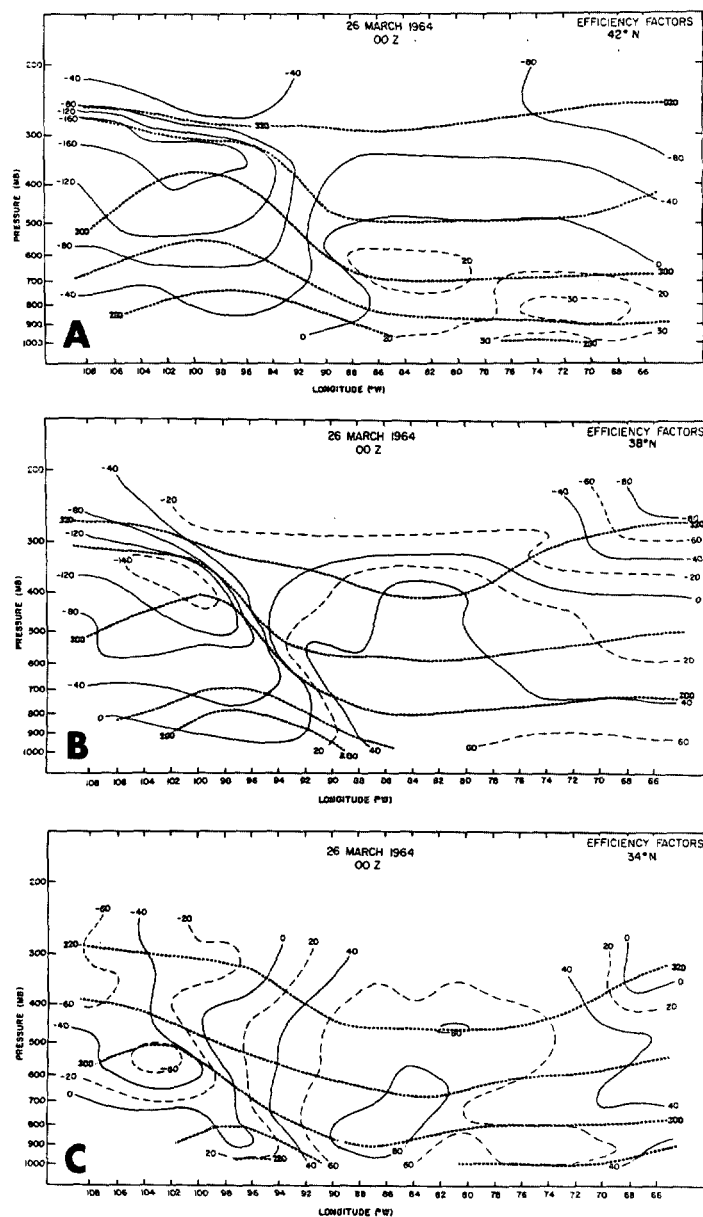


FIGURE 4.—East-west cross sections of efficiency factors (solid line, values times  $10^{-3}$ ) and potential temperature (dotted line,  $^{\circ}\text{K}$ ) for the mature stage.

### PRECIPITATION DISTRIBUTION

Precipitation rates used to establish total latent heat release are presented in figures 5A, 5C, and 5E. During the cyclogenetic stage, precipitation occurred in both the subtropical and polar air. Snow showers in the Western States resulted from upslope motion and low-level instability in the cold air. The region of maximum warm frontal precipitation extending from northeastern Missouri to western New York just north of the warm front resulted from thunderstorm activity and convective instability in the subtropical air. In some cases, snow was observed with these convective cells. The region of heaviest precipitation in northern Georgia, Alabama, and eastern Tennessee

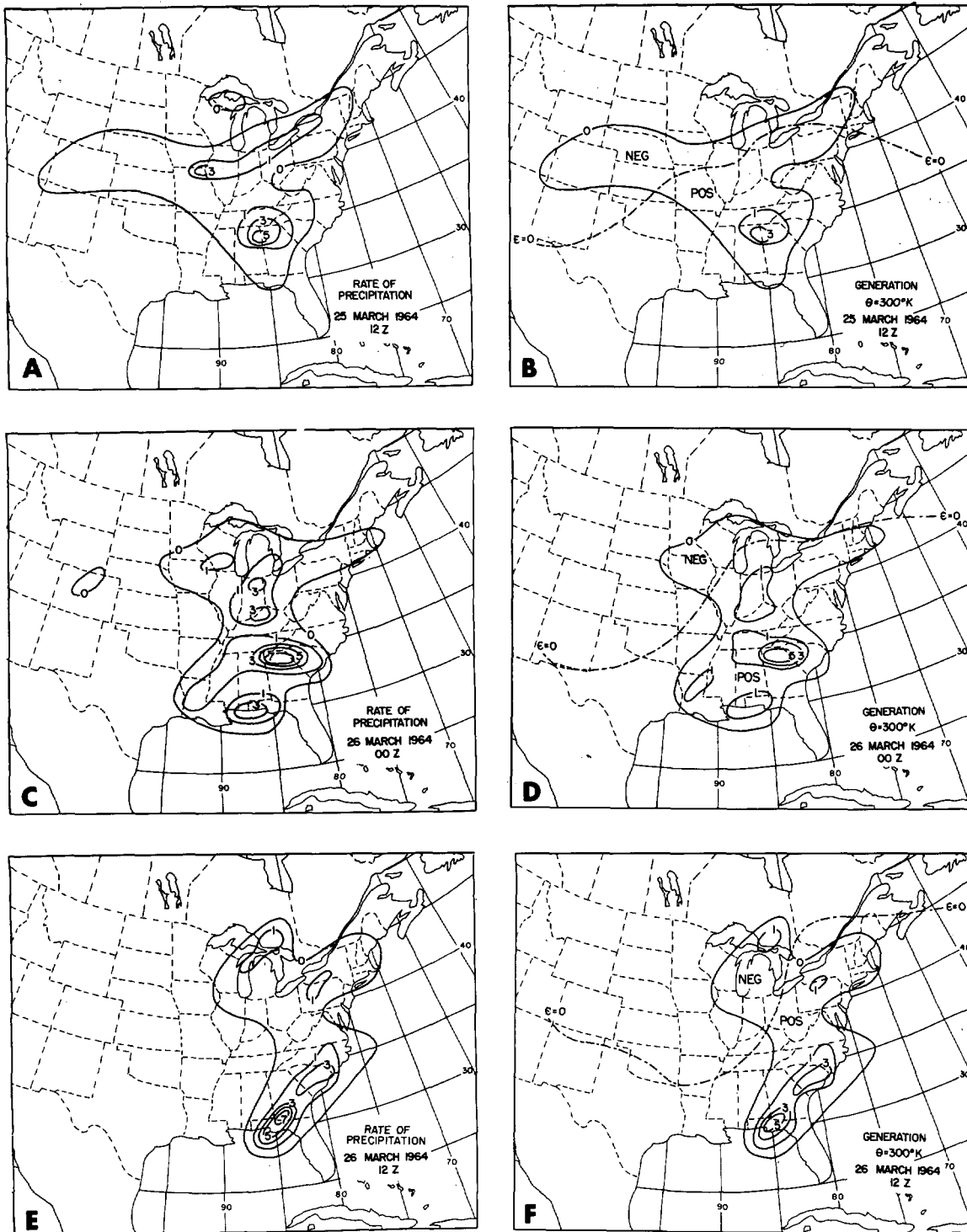


FIGURE 5.—Rate of precipitation ( $\text{mm hr}^{-1}$ ) and generation estimates ( $10^2 \text{ ergs g}^{-1} \text{ cm}^{-2} \text{ s}^{-1}$ ) on the  $300^\circ\text{K}$  surface for the cyclogenetic, mature, and occluded stages.

resulted from thunderstorms substantially ahead of the storm center in the maritime air.

During the mature stage of the storm (March 26 at 0000 GMT, fig. 5C), precipitation in the cold air north and east of the Low resulted primarily from the large-scale vertical motion field, while the areas of maximum precipitation in

the warm sector of the cyclone (fig. 2C) resulted mainly from convective activity.

By March 26 at 1200 GMT, in the beginning of the occluded stage (fig. 5E), lower precipitation rates were observed in the northern portions of the system, probably resulting from the fact that the low-level moisture source

TABLE 1.—*Estimates of the generation [watts (W) m<sup>-2</sup>] of available potential energy by latent heat release and of the frictional dissipation (W m<sup>-2</sup>) in the boundary layer*

Model of latent heat release	1		2		3			Frictional dissipation
	300	300	200	300	400			
Assumed cloud top (mb)	300	300	200	300	400			
Mar. 25, 1964, 12 (GMT)	1.0	1.0	0.7	0.9	1.1		3.1	
Mar. 26, 1964, 00	7.9	8.0	7.8	8.0	8.3		5.1	
Mar. 26, 1964, 12	6.0	6.0	5.9	6.0	6.2		9.1	

was being cut off in the occlusion process. Convective activity along the cold front produced the largest precipitation amounts in the southeastern United States.

Using all three models described in section 3, the rate of release of latent heat was computed for isentropic surfaces between the lifting condensation level and the assumed cloud top, and analyses were prepared for the 300°K surface. The distribution of latent heat release on this surface closely resembled that of the surface precipitation rates, and the analyses are not presented.

#### THE GENERATION AND FRICTIONAL DISSIPATION

Generation estimates using the three models described in section 3 were computed for the storm. A cloud top of 300 mb was assumed for the computations with models 1 and 2, while cloud tops of 200, 300, and 400 mb were used with model 3 to study the importance of vertical variations of latent heat release in generating available potential energy. The results of the computations (table 1) indicate positive generation for each stage of the storm. However, the generation during the mature and early occluded stage is nearly an order of magnitude greater than that in the cyclogenetic stage.

The small generation values for the cyclogenetic stage resulted from the conditions that precipitation tended to be slight and evenly distributed in the warm and cold air. This is evident on a comparison of the positive and negative generation areas presented in figures 5B, 5D, and 5F that illustrate the variations of the generation contribution for the three stages. Notice that the negative generation area is largest during the cyclogenetic stage and that the zone of maximum latent heat release in the northern portion of the precipitating region of the cyclogenetic stage (fig. 5B) caused little generation by virtue of its coincidence with the zero efficiency isoline. The maximum generation during the mature stage resulted from the large precipitation amounts in the cyclone's warm sector, while the slightly smaller generation in the occluded stage was associated with reduced precipitation amounts in the same region.

Estimates of the area-averaged frictional dissipation of the planetary boundary layer computed from eq (22) are presented in the last column of table 1. In the cyclogenetic

and early occluded stages, the boundary layer dissipation exceeded the generation by the latent heat component. In the mature stage, generation exceeds dissipation. The increase of the generation by the latent heat component from approximately 1.0 W m<sup>-2</sup> in the cyclogenetic stage to 8.0 W m<sup>-2</sup> in the mature stage and the excess of the generation over the frictional dissipation of 5.1 W m<sup>-2</sup> in the mature stage strongly suggests that an in situ source of energy exists within the storm that aids in its development. All of the estimates suggest that the generation by the latent heat component at the secondary scale is a significant fraction of the rate of kinetic energy dissipation within the storm.

#### VERTICAL DISTRIBUTION OF HEATING AND GENERATION

The latent heat component of the generation on an isentropic surface is largely due to the covariance between heating and the efficiency factor. The efficiency cross sections showed that the largest positive factors occur at high pressure in the subtropical air and the largest negative values occur at low pressure in the polar air. The decrease of efficiency factors with height in both polar and subtropical air indicates that the vertical variation of the heating is also important in the generation process. Vertical profiles were computed from the mass-weighted integral defined by

$$F(\theta) = \int \rho J_{\theta} f dA. \quad (24)$$

For  $f$  equal to  $Q_m$  and  $\epsilon Q_m$ , eq (24) provides profiles of latent heat release and the generation contribution as a function of potential temperature.

The physical interpretation of these profiles is difficult if one attempts to associate the heating or generation on an isentropic surface with geometric height. However, the profiles explain the relationship between isentropic structure, distribution of latent heat release, and generation.

In figure 6A, profiles of latent heat release for three stages of the cyclone are presented. These profiles were computed using the third model of latent heat release and a constant cloud top of 300 mb. The most interesting feature is the time variation of the relative maximum within the 300°–310°K layer associated with the latent heat release in the subtropical air. In the cyclogenetic stage, the maximum is somewhat lower than in the latter two stages. This difference is due to the distribution of precipitation about the storm. In the cyclogenetic stage, approximately equal amounts of precipitation fell within the warm and cold sectors. In the mature and occluded stages, a larger percentage of the total rainfall occurred in the warm sector, which contributed to latent heat release at higher potential temperatures. While profiles of heating with respect to pressure or geometric height would display a similar quadratic variation, it is doubtful

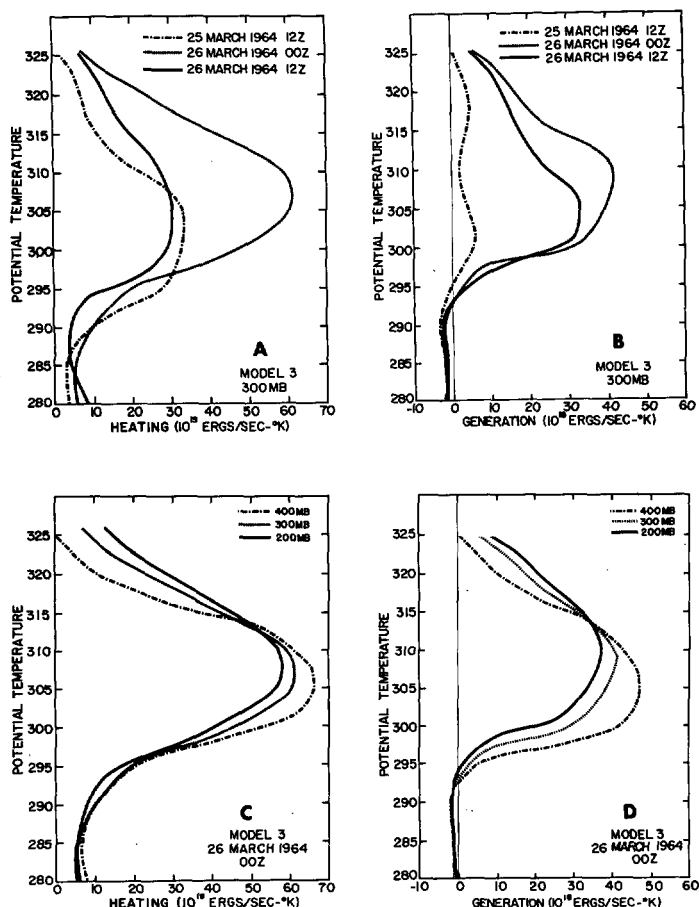


FIGURE 6.—Profiles of latent heat release and generation for the three stages from model 3 are presented in (A) and (B). Profiles of latent heat release and generation for the mature stage incorporating a variable cloud top in model 3 are presented in (C) and (D).

that the upward displacement of the relative maximum with respect to time would be detected.

The generation profiles in figure 6B confirm the importance of the vertical variation of precipitation with respect to potential temperature. While approximately the same amount of total heating occurred in the cyclogenetic and occluded stages ( $7.3 \times 10^{21}$  ergs  $s^{-1}$  vs.  $7.4 \times 10^{21}$  ergs  $s^{-1}$ ), the much smaller generation for the cyclogenetic stage resulted from the condition that more precipitation occurred in the negative efficiency region of the polar air. See the negative and positive generation areas on the  $300^\circ\text{K}$  isentropic surface for the two time periods in figures 5B and 5D. The maximum generation for the mature stage is due not only to a more favorable horizontal distribution of precipitation but also to the condition that the maximum latent heat release of  $13.1 \times 10^{21}$  ergs  $s^{-1}$  occurred for this stage.

In figure 6C, the effect of varying the cloud top parameter is shown for the mature stage. Lowering the cloud top increases the heating at lower levels but decreases it at higher levels. A similar effect is evident in the generation profiles in figure 6D. The results in table 1 show that

the total generation increases slightly with a lower cloud top height. The assumption of a constant cloud top for a cyclone is, of course, an oversimplification. In reality, the cloud tops vary, and the latent heat release is distributed within different layers of the atmosphere in various positions of the storm. However, the rather slight dependency of the generation estimates to cloud top variations indicates that the generation is not critically dependent upon this parameter in this study.

This conclusion is reinforced by the rather close agreement in generation estimates between the three models of heat release for a 300-mb cloud top. Because the profiles of latent heat release for model 1 showed a very uniform distribution with potential temperature while those of models 2 and 3 were of a quadratic nature, the agreement in generation estimates must be due to the special nature of the vertical distribution of the efficiencies. Note in figure 1A that  $Q_m$  tends to be a constant value; and in figure 1B,  $Q_m$  tends to be quadratic. If in the precipitating subregion the product of  $\epsilon$  and  $\partial p/\partial \theta$  tends to be linear, the integrated product of  $Q_m$ , constant or quadratic function, with  $\epsilon(\partial p/\partial \theta)$ , a linear function, will tend toward the same value for all three models.

While one may conclude for the diagnostic modeling that the differences in this study between models and within models are relatively unimportant for estimates of the generation of available potential energy, the same conclusion is not valid for a prognostic model in isentropic coordinates. For an isentropic model, the heating function is the "vertical motion" with respect to that coordinate system. Thus, since heating determines the vertical exchange of mass, momentum, and energy in an isentropic model, the prognostic heating profile must converge to its corresponding profile in the atmosphere for accurate numerical weather prediction.

#### TOTAL GENERATION AND FRICTIONAL DISSIPATION AS A FUNCTION OF AREA

In the results presented thus far, a circular area with a 1700-km radius about the storm center was selected for computing the reference pressure. One naturally questions whether or not changes in area will cause significant variations in estimates of the storm's generation of available potential energy. To answer this question, table 2 presents a comparison of the generation by the latent heat component in the mature stage from the third model for smaller circular areas centered about the storm. A cloud top of 400 mb was arbitrarily selected for the comparison.

The results in table 2 show that the total generation estimates for the volume decreased 18 percent when the radius of the circular area was decreased from 1700 to 1100 km. In contrast, the total boundary layer frictional dissipation decreased about 38 percent for the same change in area. The 38-percent decrease in total dissipation is due to the reduced areal extent of the boundary layer. Two factors account for the decrease in total generation. First,

TABLE 2.—Generation ( $\bar{G}$ ), frictional dissipation ( $\bar{D}$ ), total generation ( $\bar{G}A$ ), and total boundary frictional dissipation ( $\bar{D}A$ ) for various circular areas,  $A$ , about the mature stage of the storm. The cloud top is assumed to be 400 mb.

Radius (10 <sup>3</sup> km)	$A$ (10 <sup>12</sup> m <sup>2</sup> )	$\bar{G}$ (W m <sup>-2</sup> )	$\bar{D}$ (W m <sup>-2</sup> )	$\bar{G}A$ (W)	$\bar{D}A$ (W)
1.7	9.0	8.3	5.1	74.7	45.9
1.4	6.2	11.3	5.8	70.0	36.0
1.1	3.8	16.0	7.5	60.8	28.5

TABLE 3.—Total heating (10<sup>14</sup> W) and average generation (W m<sup>-2</sup>) of available potential energy by latent heat release and infrared emission for the storm volume with a 1700-km radius. Estimates from latent heat release are by the third model with a cloud top of 200 mb. Infrared estimates are: test 1, uniform ( $-1.4^{\circ}\text{C day}^{-1}$ ); test 2, clear ( $-1.6^{\circ}\text{C day}^{-1}$ ) versus cloudy ( $-1.2^{\circ}\text{C day}^{-1}$ ); test 3 clear ( $-1.8^{\circ}\text{C day}^{-1}$ ) versus cloudy ( $-1.0^{\circ}\text{C day}^{-1}$ ).

March	Time (GMT)	Total heating		Generation			
		Latent model 3	Infrared test 1	Latent model 3	Infrared		
					Test 1	Test 2	Test 3
25	12	7.3	-9.9	0.7	0.9	1.1	1.3
26	00	13.1	-10.4	7.8	1.2	1.6	2.0
26	12	7.4	-10.9	5.9	1.1	1.7	2.3

the increased reference pressures for the smaller areas tended to increase the region of negative efficiency factors; and second, the reduced areas contained less total precipitation. Fortunately, the rather small variation in total generation estimates shows that selection of the area for computing the total generation by the storm is not critical.

One extremely interesting implication of these results is evident in the estimates of mean generation. Note in table 2 that the average generation increased from 8.3 to 16.0 W m<sup>-2</sup>, a result which indicates that the energy generated is primarily available within the region where development and intensity of the storm is a maximum. Very likely at this time, the generation rate by this component exceeds the total kinetic energy dissipation within the 1100-km volume.

## 6. ESTIMATES OF THE GENERATION BY INFRARED EMISSION

While the diabatic process of latent heat release is of primary interest in this study, two simplified distributions for the divergence of infrared irradiance were also assumed to assess the possible importance of this process in generating the storm's available potential energy. For the first test, uniform heating throughout the volume of  $-1.4^{\circ}\text{C day}^{-1}$  was assumed. The rate of specific heat addition was computed by

$$Q_m = c_p \left( \frac{\partial T}{\partial t} \right)_I \quad (25)$$

where  $(\partial T/\partial t)_I$  is the instantaneous temperature change due to infrared emission. Average generation estimates for the storm volume with a 1700-km radius are presented under test 1 in table 3. Note that the average generation increased from the cyclogenetic to the mature stage and then decreased by a very small amount from the mature to the occluding stage. This trend in the estimates parallels those for latent heat release, although the magnitudes of the generation estimates by this model of infrared emission are substantially lower than those for latent heat release.

The importance of the covariant nature between a given heating distribution and the efficiency factors in generating available potential energy is evident in comparing the total heating and generation in table 3.

The order of magnitude of the total heating by the infrared and the latent heat components is the same for all stages. In the cyclogenetic stage, approximately the same generation resulted from these two processes. However, in the mature and occluding stages, the generation by latent heat release was substantially higher because the major areas of precipitation occurred in the subtropical air. The enhanced generation by latent heat release in the latter two stages is due primarily to the increase of the covariance of the efficiency and heating. For the case of uniform infrared cooling, the covariance of  $Q_m$  and  $\epsilon(\partial p/\partial \theta)$  is zero, and the positive generation results because the mass-averaged efficiency on an isentropic surface is negative. If Lorenz' (1955) isobaric approximation had been utilized, the estimate of generation from the uniform cooling would be identically zero in contrast to the isentropic estimate of approximately 1 W m<sup>-2</sup>.

Because extensive middle and upper level stratoform clouds substantially reduce the infrared cooling, two additional tests incorporating this effect were conducted. Within the volume about the storm, the clear and cloudy areas were determined from the synoptic data. Two different infrared cooling rates were then assumed to be representative. The heating rates for clear and cloudy regions for test 2 were  $-1.6^{\circ}\text{C day}^{-1}$  versus  $-1.2^{\circ}\text{C day}^{-1}$ ; and for test 3, they were  $-1.8^{\circ}\text{C day}^{-1}$  versus  $1.0^{\circ}\text{C day}^{-1}$ , respectively. Admittedly, this approach is crude, since the strong cooling at cloud tops was not incorporated in the model. Results of the generation computations are presented in table 3. The generation estimates from tests 2 and 3 are slightly greater than test 1. This increase is due to the covariance between  $Q_m$  and  $\epsilon(\partial p/\partial \theta)$  because the average of the heating remained  $-1.4^{\circ}\text{C day}^{-1}$ . However, from a comparison of the results, the generation by the latent heat component is the primary diabatic component that provides an in situ source of energy to partially offset the kinetic energy dissipation within this extratropical cyclone.

## 7. SUMMARY AND CONCLUSIONS

In this study, the generation of storm available poten-

tial energy (Johnson 1970) due to the process of latent heat release has been estimated for the cyclogenetic, a mature, and an early occluding stage of a mid-latitude cyclone. Preliminary results for the process of infrared cooling have also been presented. Three different models for the vertical distribution of latent heat release produced positive generation estimates for all stages of the storm.

Results from the third model, physically the most realistic, show that the generation is primarily dependent upon the distribution of precipitation about the cyclone. The largest generation by the latent heat component,  $6-8 \text{ W m}^{-2}$ , occurred in the latter two stages when the maximum latent heat release occurred in the cyclone's warm sector. In the cyclogenetic stage, the generation was about  $1.0 \text{ W m}^{-2}$ . Because efficiency factors for the storm tend to decrease with height, maximum condensation in the lower levels generates more available potential energy than when condensation is a maximum at higher levels.

Two simplified infrared cooling distributions produced generation estimates ranging from 1 to  $2 \text{ W m}^{-2}$ . While these results are tentative, they indicate that the process of infrared cooling contributes a smaller portion of the total generation for well-organized disturbances than for developing systems.

The fact that latent heat release produced positive generation values for all stages of the storm is significant. However, from the small generation in the developing stage, we conclude as Danard (1964) did that latent heat release alone cannot initiate the development of a storm but can provide an important source of energy for its maintenance after its circulation is established.

Of the estimates for the three stages, the generation by the latent heat component for the cyclogenetic stage is probably the most questionable. In the modeling, it was assumed that all condensed water vapor immediately precipitated. However, in a developing cyclone, it is possible that a significant percentage of the latent heat was released in the formation of the extensive cloud cover present in later stages of the cyclone. The diagnostic model of this study is incapable of estimating this contribution. Thus, one cannot conclusively state that the energy generated by the latent heat release in the incipient stage is not a factor in its early development.

The percentage error in the generation estimates in the mature and occluding stages of  $8$  and  $6 \text{ W m}^{-2}$  is likely less susceptible to errors from net condensation not precipitated. The magnitude of both estimates demonstrates the importance of latent heat release in well-organized synoptic systems. The time variations from 1 to  $8$  to  $6 \text{ W m}^{-2}$  for the three stages indicate that the in situ source of energy available for conversion to kinetic energy by the latent heat release is an important factor in the transient behavior of the storm. The estimates of boundary layer frictional dissipation by Lettau's (1961) model from the surface pressure gradient shows that dissipation increases from 3 to 5 to  $9 \text{ W m}^{-2}$  during the three stages. In contrast, the generation by the latent

heat release and infrared emission reached its maximum intensity during the mature stage, being nearly twice the dissipation. It decreased by  $2 \text{ W m}^{-2}$  from the mature to the early occluding stage. From the condition that the storm's low-level moisture supply will continue to be reduced in the occluding process and more latent heat will be released in the cold core vortex of the occluded system, very likely the generation will continue to decrease. The results of this study indicate that the decrease in the generation precedes and likely exceeds the decrease of kinetic energy dissipation in the storm. Thus, the implication that the in situ energy generated by the latent heat release to offset kinetic energy dissipation may be an important factor in the transient behavior of the disturbance is extremely interesting.

The results of this study compare favorably with those obtained by Danard (1966). Using Lorenz' approximate equation, involving the covariance of isobaric deviations of temperature and heating, Danard obtained a generation of approximately  $11 \text{ W m}^{-2}$  for a region containing a rapidly developing extratropical cyclone. Because a large portion of the precipitation occurred in the warm sector of the cyclones used for both this and Danard's study, the agreement between results re-emphasizes the importance of the distribution of precipitation in generating available potential energy at the storm scale. The distribution of precipitation about the storm studied here is not typical of all extratropical cyclones. Many have relatively dry warm sectors with major precipitation areas north of the warm front. The generation by latent heat release within these systems is probably less. Further studies are needed to clarify the role of diabatic processes within extratropical cyclones.

The interaction energetically of the middle-latitude cyclone with the circumpolar vortex during the growth, maturation, and decay of the storm is an unsolved problem. The results of this investigation that the in situ generation of the storm is transient, at times being large and being sufficient to offset a major portion of the local frictional dissipation of the system, represents another step in the search for the energy sources of the extratropical cyclone.

#### ACKNOWLEDGMENTS

The research was jointly supported by the National Environmental Satellite Center, Environmental Science Services Administration, ESSA Grants WBG-52 and E-8-69(G), and the Atmospheric Sciences Section, National Science Foundation, NSF Grant GA-10997. Partial support was provided by the Wisconsin Alumni Research Foundation and the National Science Foundation in the form of a grant for computational funds and the use of computer facilities.

#### REFERENCES

- Aubert, Eugene J., "On the Release of Latent Heat as a Factor in Large Scale Atmospheric Motions," *Journal of Meteorology*, Vol. 14, No. 6, Dec. 1957, pp. 527-542.

- Bradbury, Dorothy L., "An Experiment in Stability and Moisture Analysis," *Final Report*, Contract AF19(604)-1293, Department of Meteorology, University of Chicago, Feb. 1957, 32 pp.
- Danard, Maurice B., "On the Influence of Released Latent Heat on Cyclone Development," *Journal of Applied Meteorology*, Vol. 3, No. 1, Feb. 1964, pp. 27-37.
- Danard, Maurice B., "On the Contribution of Released Latent Heat to Changes in Available Potential Energy," *Journal of Applied Meteorology*, Vol. 5, No. 1, Feb. 1966, pp. 81-84.
- Dutton, John A., and Johnson, Donald R., "The Theory of Available Potential Energy and a Variational Approach to Atmospheric Energetics," *Advances in Geophysics*, Vol. 12, 1967, pp. 333-436.
- Eliassen, Arnt, "On the Vertical Circulation in Frontal Zones," *Geofysiske Publikasjoner*, Vol. 24, Oslo, 1962, pp. 147-160.
- Hahn, D., and Horn, Lyle, "The Generation of Available Potential Energy in a Mid-Latitude Cyclone," *Studies of Large Scale Atmospheric Energetics, Final Report*, ESSA Grant WBG-52, Department of Meteorology, The University of Wisconsin, Madison, June 1969, pp. 1-56.
- Johnson, Donald R., "The Available Potential Energy of Storms," *Journal of the Atmospheric Sciences*, Vol. 27, No. 5, Sept. 1970, pp. 727-741.
- Kung, Ernest C., "Climatology of Aerodynamic Roughness Parameter and Energy Dissipation in the Planetary Boundary Layer Over the Northern Hemisphere," *Annual Report*, Contract DA-36-039-AMC-00878, Department of Meteorology, The University of Wisconsin, Madison, Nov. 1963, pp. 37-96.
- Lettau, Heinz H., "Theoretical Wind Spirals in the Boundary Layer of a Barotropic Atmosphere," *Annual Report*, Contract No. DA-36-039-80282, Department of Meteorology, The University of Wisconsin, Madison, Aug. 1961, pp. 115-170.
- Lorenz, Edward N., "Available Potential Energy and the Maintenance of the General Circulation," *Tellus*, Vol. 7, No. 2, May 1955, pp. 157-167.
- Lorenz, Edward N., "The Nature and Theory of the General Circulation of the Atmosphere," *WMO Bulletin*, Vol. 16, No. 2, World Meteorological Organization, Geneva, Apr. 1967, pp. 74-78.
- Margules, Max, "Über die Energie der Stürme" (On the Energy of Storms), *Jahrbuch Zentralamt für Meteorologie und Geodynamik*, Vol. 40, Vienna, 1903, 26 pp.
- Petterssen, Sverre, "On the Influence of Heat Exchanges on Motion and Weather Systems," *Final Report*, Contract No. AF19(604)-2179, Department of Meteorology, The University of Chicago, Feb. 1960, 18 pp.
- Rao, Gandikota V., "On the Influences of Fields of Motion, Baroclinicity and Latent Heat Source on Frontogenesis," *Journal of Applied Meteorology*, Vol. 5, No. 4, Aug. 1966, pp. 377-387.
- Starr, Victor P., "What Constitutes Our New Outlook on the General Circulation?," *Journal of the Meteorological Society of Japan*, Ser. II, Vol. 36, No. 5, Oct. 1958, pp. 167-173.
- Wexler, Raymond, and Atlas, David, "Moisture Supply and Growth of Stratiform Precipitation," *Journal of Meteorology*, Vol. 15, No. 6, Dec. 1958, pp. 531-538.

[Received February 24, 1970; revised May 13, 1970]